

A new model for turbidity current behavior based on integration of flow monitoring and precision coring in a submarine canyon

William O. Symons^{1*}, Esther J. Sumner¹, Charles K. Paull², Matthieu J.B. Cartigny³, J.P. Xu⁴, Katherine L. Maier⁵, Thomas D. Lorenson⁵, and Peter J. Talling³

¹School of Ocean and Earth Science, University of Southampton, National Oceanography Centre, Southampton SO14 3ZH, UK

²Monterey Bay Aquarium Research Institute, Moss Landing, California 95039, USA

³Departments of Earth Science and Geography, University of Durham, Durham DH1 3LY, UK

⁴College of Marine Geosciences, Ocean University of China, Qingdao 266100, China

⁵U.S. Geological Survey, Pacific Coastal and Marine Science Center, Santa Cruz, California 95060, USA

ABSTRACT

Submarine turbidity currents create some of the largest sediment accumulations on Earth, yet there are few direct measurements of these flows. Instead, most of our understanding of turbidity currents results from analyzing their deposits in the sedimentary record. However, the lack of direct flow measurements means that there is considerable debate regarding how to interpret flow properties from ancient deposits. This novel study combines detailed flow monitoring with unusually precisely located cores at different heights, and multiple locations, within the Monterey submarine canyon, offshore California, USA. Dating demonstrates that the cores include the time interval that flows were monitored in the canyon, albeit individual layers cannot be tied to specific flows. There is good correlation between grain sizes collected by traps within the flow and grain sizes measured in cores from similar heights on the canyon walls. Synthesis of flow and deposit data suggests that turbidity currents sourced from the upper reaches of Monterey Canyon comprise three flow phases. Initially, a thin (38–50 m) powerful flow in the upper canyon can transport, tilt, and break the most proximal moorings and deposit chaotic sands and gravel on the canyon floor. The initially thin flow front then thickens and deposits interbedded sands and silty muds on the canyon walls as much as 62 m above the canyon floor. Finally, the flow thickens along its length, thus lofting silty mud and depositing it at greater altitudes than the previous deposits and in excess of 70 m altitude.

INTRODUCTION

Turbidity currents are energetic gravity-driven flows that dominate sediment transport across large expanses of seafloor and play an important role in global carbon burial. Turbidity currents can break seafloor cables (e.g., Grand Banks; Heezen and Ewing, 1952; Piper et al., 1999) and pipelines, resulting in millions of dollars being spent rerouting pipelines (e.g., Cooper et al., 2013). The fundamental nature of turbidity currents is poorly understood because of a paucity of direct observations that results from difficulties in measuring these often destructive flows (Xu, 2010; Liu et al., 2012). As a result, most of our understanding of turbidity currents results from interpreting the deposits that they leave behind in the sedimentary record (e.g., Pirmez and Imran, 2003; Talling et al., 2012; Hubbard et al., 2014). However, the validity of such interpretations remains controversial due to a lack of field data sets that include both flow and deposit measurements (e.g., Puig et al., 2004; Khripounoff et al., 2009).

This study is novel because it combines some of the most detailed direct measurements from turbidity currents (Xu et al., 2004, 2014) with a new set of precisely located core transects through their deposits. We extend the previous analysis of monitoring data by Xu et al. (2004, 2014) by also documenting patterns of mooring tilt and movement. We show that the new cores contain the monitored flows, although age control does not allow individual deposits to be linked to specific flows. The aims of this study are to evaluate how well deposits record flow properties and produce a new model of turbidity current evolution that combines both flow measurements and deposits.

Characteristics of Turbidity Currents in Monterey Canyon Based on Monitoring Studies

Multiple turbidity currents occur in Monterey Canyon (offshore California, USA) each year (Xu et al., 2004; Paull et al., 2010). It is rare for turbidity currents in this canyon to extend beyond 2000 m water depth (Xu, 2011); the last event to pass Shepard Meander (3400 m water depth, 36°13'00"N, 122°52'00"W) occurred

150 yr ago (Johnson et al., 2005). Most flows have not been monitored in detail, but are known to have occurred because they damaged seafloor equipment (e.g., Paull et al., 2010). Only four turbidity currents have been previously monitored in detail and at multiple locations in Monterey Canyon (Xu et al., 2004, 2014; Xu, 2010). These turbidity currents were monitored using three U.S. Geological Survey moorings located in the canyon thalweg at water depths of 820 m (R1), 1020 m (R2), and 1445 m (R3) that were deployed from December 2002 to November 2003 (Fig. 1) (Xu et al., 2004). While the instruments were only deployed for 12 months, this is the best available data set to assess the characteristics of turbidity currents in Monterey Canyon and how much variability exists among flows. These data sets are probably typical of the frequency of small events that fill the canyon; larger flows must occasionally occur that flush sediments onto the submarine fan.

Three of the four turbidity currents originated in Monterey Canyon, and one flow was sourced from Soquel Canyon (a tributary of Monterey Canyon; Fig. 1). The turbidity current from Soquel Canyon exhibits different characteristics (Xu et al., 2004, 2014), probably because Soquel Canyon sediment is finer grained than that of Monterey Canyon (Paull et al., 2005). We therefore focus our analyses on the three turbidity currents sourced from Monterey Canyon. All of these three turbidity currents had a thin flow front at the shallowest mooring and thickened through time and downstream, as shown by Xu (2010). The thin flow front was evident at the second mooring but not at the deepest mooring. The longevity of this thin flow front varied from 1 to 6 h among the different flows (Table DR3 in the GSA Data Repository¹). The maximum thickness of the flows was 48–59

¹GSA Data Repository item 2017105, supplemental methods and discussion, including Figures DR1–DR9 and Tables DR1–DR3, is available online at <http://www.geosociety.org/datarepository/2017/> or on request from editing@geosociety.org.

*E-mail: w.o.symons@soton.ac.uk

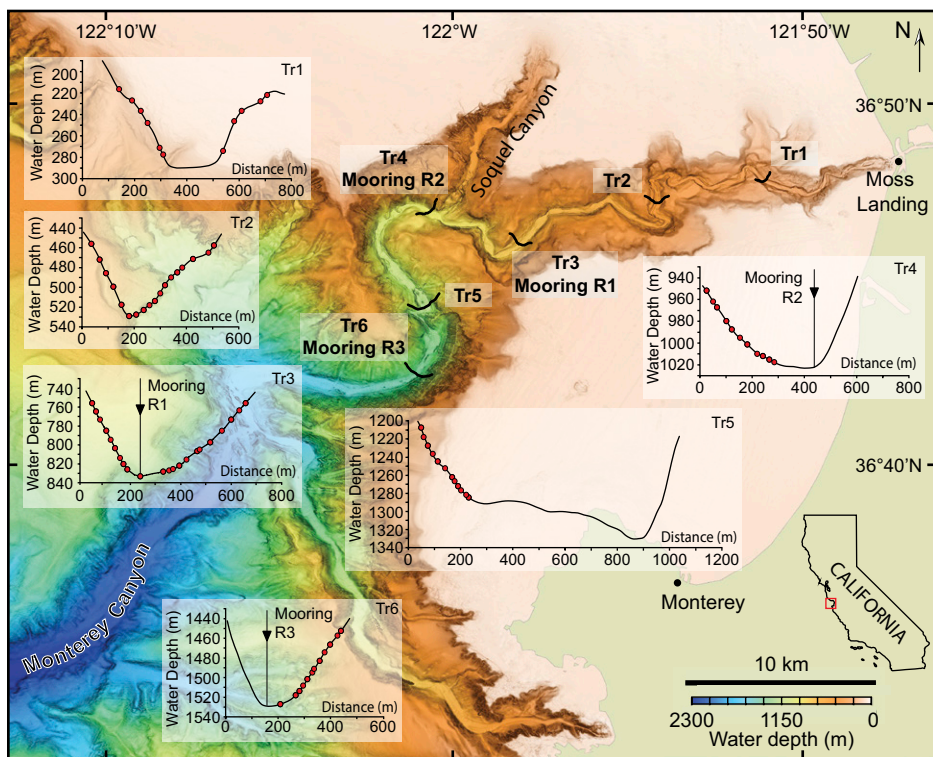


Figure 1. Map showing the bathymetry of Monterey Bay, offshore California (USA) (modified after Paull et al., 2010). Included are the locations and cross sections (looking down-canyon with core locations) of Monterey Canyon at transects Tr1–Tr6. The positions of moorings R1–R3 and sediment traps (inverted triangles) are shown on transects Tr3, Tr4, and Tr5.

m. The 3 turbidity currents had broadly comparable maximum hourly velocities of 1–2 m s⁻¹ at each mooring (Table DR3). The run-out distances of the turbidity currents are variable: two of the flows pass all moorings, whereas the second Monterey Canyon flow did not reach the deepest mooring.

We now focus on the second turbidity current (TC2) from Monterey Canyon because it was the only event captured at all three moorings and is the only event from Monterey Canyon with grain-size data from sediment traps. This turbidity current is intermediate in thickness between the two other flows. The speeds and dimensions of the other two flows are summarized in Table DR3.

METHODS

In April and October 2014, core transects (Tr) were collected in Monterey Canyon at water depths of 275 (Tr1), 530 (Tr2), 830 (Tr3), 1020 (Tr4), 1280 (Tr5), and 1525 m (Tr6) (Fig. 1). Data were collected using a 25-cm-long push corer deployed from Monterey Bay Aquarium Research Institute’s remotely operated vehicle (ROV) *Doc Ricketts*. This ROV-deployed coring system enables location of cores at different heights above the thalweg to a level of precision that cannot be achieved using traditional wireline coring techniques. Across-canyon transects comprised as many as 12 push cores and included samples from the thalweg, terraces

(raised plateaus between the incised thalweg and canyon wall), and the canyon walls up to an altitude of 70 m above local thalweg (m-alt) (Fig. 1). The facies in the push cores were visually analyzed and then sampled for grain-size and ²¹⁰Pb analyses. Grain-size analyses were conducted using the same laser particle size analyzer used for the A.D. 2002 sediment trap data (Xu et al., 2014).

The flow measurements and samples were collected 12 yr apart. We do not aim to identify the precise deposits laid down by the flows in 2002–2003. Instead, we use ²¹⁰Pb analysis to assess whether the time interval represented by the cores encompasses the time period from 2002 to 2003 and note that deposit characteristics are consistent throughout the depth of each core.

RESULTS

Sedimentary Facies

The push cores contain the following five sedimentary facies (see the Data Repository). (1) **Indurated substrate** is firm mud that may be homogeneous or contain rip-up clasts. (2) **Chaotic sand and gravel** comprises poorly sorted clean sands and gravel overlain by a soft mud drape. (3) **Clean sands** are moderately to well-sorted fine- to medium-grained sands that may be ungraded or normally graded. (4) **Interbedded sand and silty mud** comprises fine sands interbedded with silty mud; the sand laminae

and/or beds range in thickness from 0.5 to 6 cm. (5) **Silty mud** comprises homogeneous or bioturbated silty mud.

Facies Distribution from Push Core Transects

We here describe the lithofacies seen in transects (Tr) of cores collected along canyon floors and walls (Fig. 2B).

Tr1. No recent deposits are seen below 40 m-alt, instead indurated substrate is recorded on the steep (~27°) canyon walls; silty mud crops out at 40 m-alt (Fig. 2B). The maximum grain size recorded on the canyon walls is 200 μm. Previous studies have identified chaotic sand and gravel within the thalweg (Paull et al., 2010).

Tr2. Clean sands with grain sizes to 500 μm crop out up to 6 m-alt; above 6 m-alt, interbedded sand and silty mud crop out, with silty mud higher than 29 m-alt (Fig. 2B).

Tr3. This is the first location where coincident flow measurements and deposit samples exist. Chaotic sand and gravel and clean sand, with grain sizes to 600 μm, crop out up to 1.5 and 7.5 m-alt, respectively. Above this, interbedded sand and silty mud crop out up to 35 m-alt, with silty mud reaching 75 m-alt (Fig. 2B).

Tr4. Chaotic sand and gravel and clean sand, with grain sizes to 500 μm, crop out at 2 and 4.5 m-alt, respectively. Interbedded sand and silty mud crops out at 48.5 m-alt, above which silty mud crops out (Fig. 2B).

Tr5. At Tr5 there are no chaotic sand and gravel or clean sand facies. Interbedded sand and silty mud with a maximum grain size of 300 μm crops out at 62 m-alt. Above this, silty mud crops out (Fig. 2B).

Tr6. At the most distal transect (Tr6), no coarse-grained facies are present. Interbedded sand and silty mud with a maximum grain size of 200 μm crops out at 30 m-alt with silty mud above this to 74 m-alt (Fig. 2B).

Do the Push Cores Contain Deposits from the 2002–2003 Flow Events?

²¹⁰Pb dating was used to establish the time interval represented by deposits in the push cores. Most ²¹⁰Pb profiles show non-steady-state deposition; where steady-state deposition occurred (Tr4) a sedimentation rate of 0.24 cm yr⁻¹ is calculated (Fig. DR3). Identifying specific turbidity current deposits from 2002–2003 in the cores is beyond the resolution of the dating technique. However, based on sedimentation rates, the sediments in these cores include the time period between 2002 and 2003. Furthermore, these cores have similar characteristics throughout their depth.

Comparison of Grain Sizes in Sediment Traps and Canyon-Wall Deposits

At the two deeper moorings (R2, Tr4; R3, Tr6) the sediment trap and push cores from 70

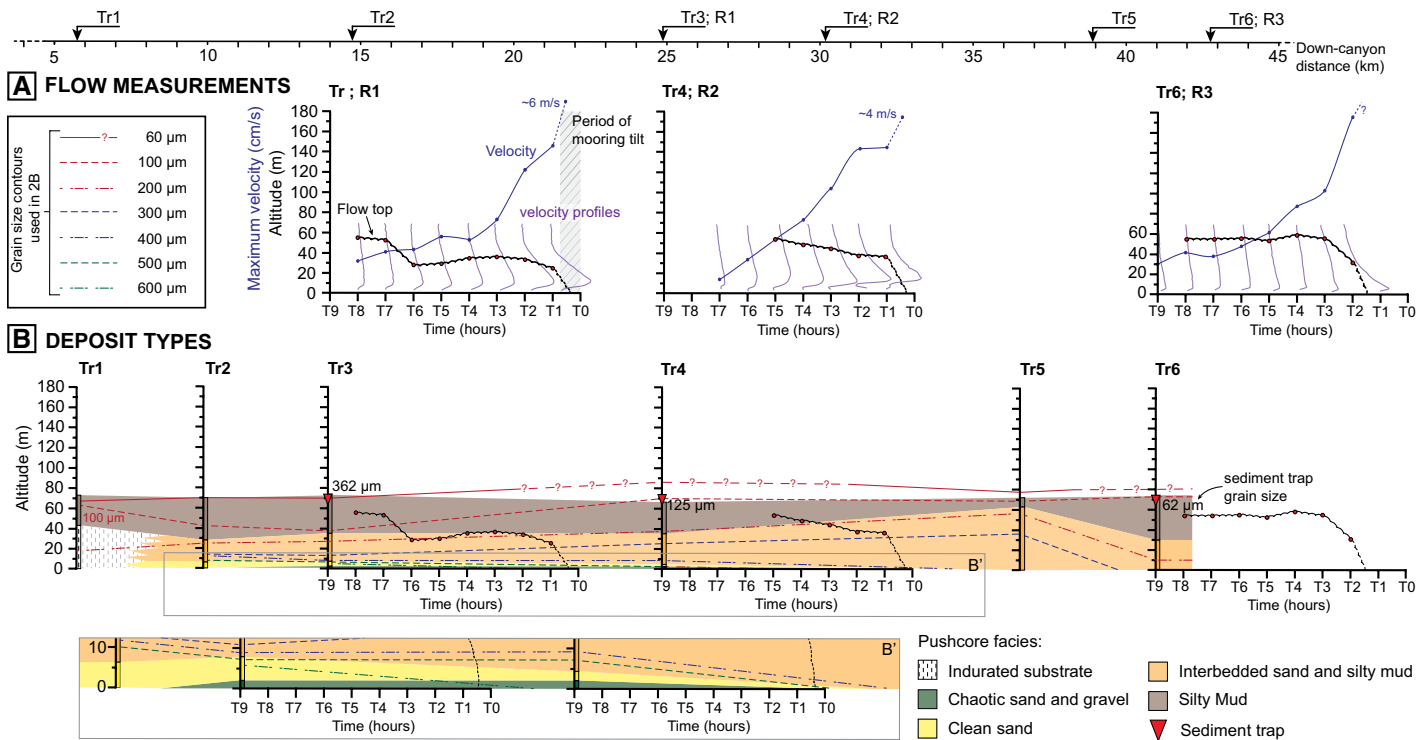


Figure 2. Summary plots for flow monitoring, grain size, and facies data. **A:** Flow monitoring data corresponding to transects Tr3, Tr4, and Tr6 showing the turbidity current thickness (black line). The maximum hourly velocity for each measurement (blue line) shows decaying velocity with time. The inferred maximum velocities (4–6 m s⁻¹) are taken from the turbidity current arrival times at the moorings. The maximum frontal velocity based on turbidity current arrival time at each mooring is stated. **B:** Grain size (dashed line) and facies distribution for the six transects. **B'** shows detail of the facies and grain sizes in the bottom 10 m.

m-alt show similar grain sizes: (1) the R2 sediment trap contains grains up to 125 μm and the canyon wall has grains up to 100 μm ; (2) the R3 sediment trap contains grains up to 62 μm and the canyon wall has grains up to 100 μm . However, at the shallow mooring (R1, Tr3) there is a discrepancy between grain sizes in the sediment trap versus in the push core at 70 m altitude; the sediment trap contains grains up to 362 μm from TC2, whereas the canyon wall has grains up to 60 μm .

Tilting and Movement of the Sediment Trap and Its Implications

Here we demonstrate that during the first ~15 min of TC2, the shallow mooring (R1, Tr3) was severely tilted and therefore collected coarse sediment from lower parts of the flow, explaining the disparity between grain sizes in the sediment trap and the canyon wall at Tr3. During the first 20 min of TC2 the pressure recorded on the mooring at 170 m above seafloor (masf) increased from 657 dbar to 675 dbar, where it remained. This pressure increase represents the mooring moving ~580 m down the canyon at ~0.5 m s⁻¹ (see the Data Repository), despite having a 1000 kg anchor (Xu et al., 2004). To further investigate the movement of the mooring we analyzed the temperature sensors, which have a higher sampling resolution (5 min) than the pressure sensors (20 min). At the onset of TC2

there was an ~15 min decrease in temperature at sensors located at 170 and 300 masf, implying that both sensors were exposed to deeper, colder water. The measured decrease in temperature suggests that the sediment trap located at 70 masf underwent a depth increase of ~37 m, allowing it to sample lower, coarser parts of the turbidity current. Thus the mooring appears to have tilted and then returned to an upright position during the first 15 min of the flow, which is prior to the first measurement by the acoustic Doppler current profiler (ADCP; sampling at an hourly rate); as a result, ADCP measurements used to define the flow structure are not compromised. The pressure and temperature sensors on moorings R2 and R3 show no evidence for tilting.

DISCUSSION

Link between Flow Structure and Deposits

We here examine the distribution of facies and relate them to different flow phases. Chaotic sands and gravels are present at very low altitudes above the thalweg (<7.5 m-alt) at Tr1–Tr4; they are not found at Tr5. Chaotic sands and gravels pinch out at a similar location to where the flows change from having a thin flow to a thick flow front (Fig. 3). They are therefore most likely linked to a high-energy, high-concentration flow phase responsible for moving the mooring. Previous studies (e.g., Paull et al.,

2005) that used longer cores have shown that these coarser facies are found at deeper depths beneath the seafloor both here and downstream, demonstrating that larger flows, that have not occurred in the past 12 yr, can produce this facies at this location and downstream.

Interbedded sand and silty muds crop out at Tr2–Tr5. The height at which this facies is recorded on the canyon walls progressively increases from 29 m to 62 m-alt between Tr2 and Tr5. This is coincident with where the turbidity currents expand and become more dilute. These deposits are indicative of a turbulent flow phase that is sufficiently dilute to enable grain segregation. These results suggest that key features of turbidity currents, such as changes in flow thickness and concentration, are faithfully recorded by their deposits.

Summary Model: Evolving Flow Structure and Resulting Deposits

We provide flow and deposit data for field-scale turbidity currents from the same location. The combined flow data (Xu et al. 2014) and deposit data suggest that there is a strong link between changes in facies and grain size on the canyon walls and measured changes in the flow structure. In addition, the combined data provide valuable insights into the dynamics of turbidity currents (Fig. 3). Monterey Canyon turbidity currents begin as thin, high-concentration highly

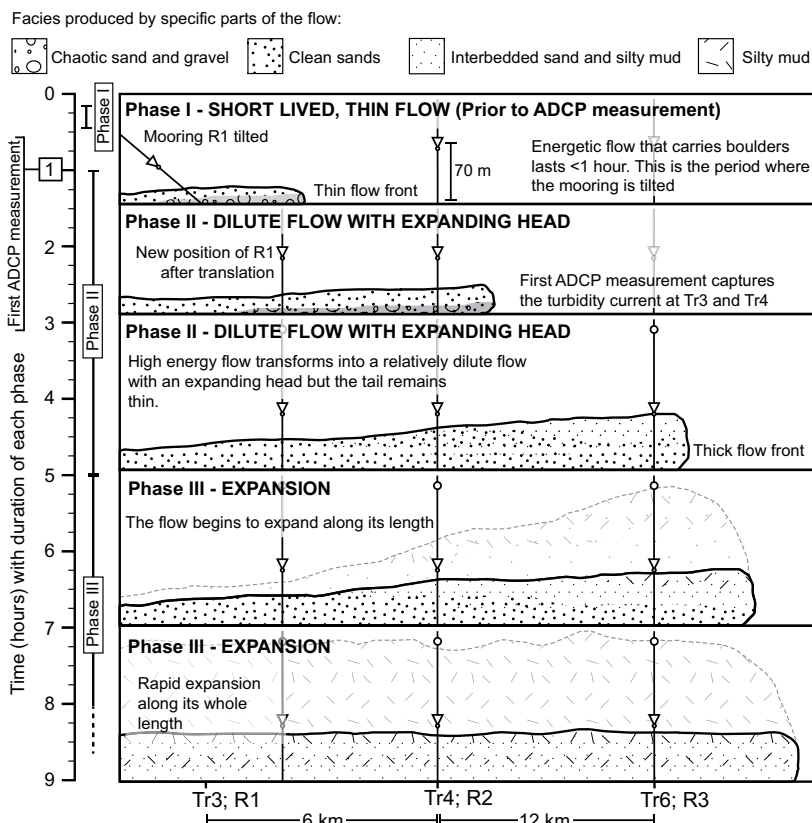


Figure 3. Interpretive diagram showing the evolution of flow structure and composition among the three moorings. Each panel shows a snapshot in time constructed using the flow thickness and facies from Figure 2. Dashed gray line on panels T5 and T7 represents the possible extent of suspended fine-grained material from saturation of transmissometers suspended at 170 m above seafloor on each mooring. ADCP—acoustic Doppler current profiler.

energetic flows that deposit chaotic sand and gravel and clean sand facies (Fig. 3). This flow phase lasts for a maximum of 1 h but is most energetic during the first 15 min when it has an estimated velocity of 4–6 m s⁻¹ (based on turbidity current arrival times at each mooring; Xu et al., 2014), which is sufficient to move a 1000 kg mooring down the canyon. This highly energetic, high-concentration phase transforms into a more dilute flow phase over the first ~30 km of the canyon and deposits interbedded sand and silty mud facies (Fig. 3). As the dilute flow travels down the canyon the head of the flow progressively thickens, resulting in interbedded sand and silty mud facies being deposited at increasingly high altitudes on the canyon walls (Fig. 3). After 5–6 h the flows rapidly thicken along their entire length, lofting and depositing silty mud (Fig. 3).

CONCLUSIONS

Broadly comparable grain sizes in sediment traps located within the flow, and in cores from similar heights on the canyon walls, increase confidence in reconstructions of flow properties from deposit textures. A novel combination of direct measurements and cored deposits provides a new three-part model of turbidity current

behavior: (1) they begin as a short-lived (at least 15 min) but highly energetic, high-concentration, thin flows; (2) they evolve into a dilute flow with an expanding head capable of transporting sand for 1–5 h; and (3) they undergo expansion along their entire length, lofting silt and depositing it high on the canyon walls. This new model has important wider implications; it suggests that the initial period of powerful flow that is most hazardous for seafloor pipelines and cable may be of limited (15–60 min) duration.

ACKNOWLEDGMENTS

Symons is funded by Natural Environment Research Council Studentship NE/L501657/1. The David and Lucile Packard Foundation provided support. We thank the crew of the R/V *Western Flyer*, the pilots of ROV *Doc Ricketts*, Angela Tan for laboratory assistance, and A. Fildani, P. Puig, and one anonymous reviewer for their reviews.

REFERENCES CITED

Cooper, C., Wood, J., and Andrieux, A., 2013, Turbidity current measurements in the Congo Canyon: Offshore Technology Conference OTC-23992-MS, p. 12, doi:10.4043/23992-MS.

Heezen, B.C., and Ewing, M., 1952, Turbidity currents and submarine slumps, and the 1929 Grand Banks earthquake: *American Journal of Science*, v. 250, p. 849–873, doi:10.2475/ajs.250.12.849.

Hubbard, S.M., Covault, J.A., Fildani, A., and Romans, B.W., 2014, Sediment transfer and deposition in slope channels: Deciphering the record of enigmatic deep-sea processes from outcrop: *Geological Society of America Bulletin*, v. 126, p. 857–871, doi:10.1130/B30996.1.

Johnson, J.E., Paull, C.K., Normark, W.R., and Ussler, W., 2005, Late Holocene turbidity currents in Monterey Canyon and fan channel: Implications for interpreting active margin turbidite records: *Eos (Transactions, American Geophysical Union)*, v. 86, abs. OS21A–1521.

Khripounoff, A., Vangriesheim, A., Crassous, P., and Etoubleau, J., 2009, High frequency of sediment gravity flow events in the Var submarine canyon (Mediterranean Sea): *Marine Geology*, v. 263, p. 1–6, doi:10.1016/j.margeo.2009.03.014

Liu, J.T., Wang, Y.-H., Yang, R.J., Hsu, R.T., Kao, S.-J., Lin, H.-L., and Kuo, F.H., 2012, Cyclone-induced hyperpycnal turbidity currents in a submarine canyon: *Journal of Geophysical Research*, v. 117, C04033, doi:10.1029/2011JC007630.

Paull, C.K., Mitts, P., Ussler, W., Keaten, R., and Greene, H.G., 2005, Trail of sand in upper Monterey Canyon: Offshore California: *Geological Society of America Bulletin*, v. 117, p. 1134–1145, doi:10.1130/B25390.1.

Paull, C.K., Ussler, W., Caress, D.W., Lundsten, E.M., Covault, J.A., Maier, K.L., Xu, J.P., and Augenstein, S., 2010, Origins of large crescent-shaped bedforms within the axial channel of Monterey Canyon, offshore California: *Geosphere*, v. 6, p. 755–774, doi:10.1130/GES00527.1.

Piper, D.J.W., Cochonat, P., and Morrison, M.L., 1999, The sequence of events around the epicentre of the 1929 Grand Banks earthquake: initiation of debris flows and turbidity currents inferred from sidescan sonar: *Sedimentology*, v. 46, p. 79–97, doi:10.1046/j.1365-3091.1999.00204.x.

Pirmez, C., and Imran, J., 2003, Reconstruction of turbidity currents in Amazon Channel: *Marine and Petroleum Geology*, v. 20, p. 823–849, doi:10.1016/j.marpetgeo.2003.03.005.

Puig, P., Ogston, A.S., Mullenbacj, B.L., Nittrouer, C.A., Parsons, D., and Sternberg, R.W., 2004, Storm-induced sediment gravity flows at the head of the Eel submarine canyon, northern California margin: *Journal of Geophysical Research*, v. 109, C03019, doi:10.1029/2003JC001918.

Talling, P.J., Masson, D.G., Sumner, E.J., and Malguesini, G., 2012, Subaqueous sediment density flows: Depositional processes and deposit types: *Sedimentology*, v. 59, p. 1937–2003, doi:10.1111/j.1365-3091.2012.01353.x.

Xu, J.P., 2010, Normalized velocity profiles of field-measured turbidity currents: *Geology*, v. 38, p. 563–566, doi:10.1130/G30582.1.

Xu, J.P., 2011, Measuring turbidity currents in submarine canyons: Technological and scientific progress in the past 30 years: *Geosphere*, v. 7, p. 868–876, doi:10.1130/GES00640.1.

Xu, J.P., Noble, M.A., and Rosenfeld, L.K., 2004, In-situ measurements of velocity structure within turbidity currents: *Geophysical Research Letters*, v. 31, p. 1–4, doi:10.1029/2004GL019718.

Xu, J.P., Sequeiros, O.E., and Noble, M.A., 2014, Sediment concentrations, flow conditions, and downstream evolution of two turbidity currents, Monterey Canyon, USA: Deep-sea Research. Part I, *Oceanographic Research Papers*, v. 89, p. 11–34, doi:10.1016/j.dsr.2014.04.001.

Manuscript received 24 June 2016

Revised manuscript received 22 December 2016

Manuscript accepted 28 December 2016

Printed in USA